

A Theoretical Comparison of Two Possible Shape Memory Processes in Shape Memory Alloy Reinforced Metal Matrix Composite

Jae Kon Lee*, Gi Dae Kim

*School of Mechanical and Automotive Engineering, Catholic University of Daegu,
Gyeongsansi, Gyeongbuk 712-702, Korea*

Two possible shape memory processes, austenite to detwinned martensite transformation and twinned martensite to detwinned martensite transformation of a shape memory alloy have been modeled and examined. Eshelby's equivalent inclusion method with Mori-Tanaka's mean field theory is used for modeling of the shape memory processes of TiNi shape memory alloy reinforced aluminum matrix composite. The shape memory amount of shape memory alloy, plastic strain and residual stress in the matrix are computed and compared for the two processes. It is shown that the shape memory amount shows differences in a small prestrain region, but the plastic strain and the residual stress in the matrix show differences in the whole prestrain region. The shape memory process with initially martensitic state of the shape memory alloy would be favorable to the increase in the yield stress of the composite owing to the large compressive residual stress and plastic strain in the matrix.

Key Words : Shape Memory Processes, Shape Memory Alloy, Fiber Reinforced Composites, Prestrain, Residual Stress, Plastic Strain

Nomenclature

General

$\langle \sigma \rangle_f$: Average stress in the fiber
 $\langle \sigma \rangle_m$: Average stress in the matrix
 σ_o : Applied stress
 Ω : Fiber domain
 D : Composite domain
 e : Strain disturbed by the existence of the inhomogeneity
 \bar{e} : Average elastic strain in the matrix
 e^* : Equivalent eigenstrain of the equivalent inclusion
 e_c : Total strain in the composite
 e_f : Total strain in the fiber

e_m : Total strain in the matrix
 e_o : Strain generated in the matrix without the inhomogeneity by applied stress
RFRE : Matrices for expressing the average fiber and matrix stresses
 S : Eshelby tensor
 T : Temperature

Shape memory alloys

ε^{TR} : Transformation strain along fiber direction
 ν_f : Poisson's ratio of the fiber
 σ_{dmf} : Critical stress at the finish of the conversion of the martensitic variants
 σ_{ams} : Critical stress at the start of the conversion of the martensitic variants
 σ_f : Effective stress of SMA fiber
 ξ_{A-DTM} : Volume fraction of detwinned martensite transformed from austenite
 ξ_{TM-DTM} : Volume fraction of detwinned martensite transformed from twinned martensite

* Corresponding Author,
E-mail : leejk@cu.ac.kr
TEL : +82-53-850-2720; **FAX :** +82-53-850-2710
 School of Mechanical and Automotive Engineering,
 Catholic University of Daegu, Gyeongsansi, Gyeongbuk
 712-702, Korea. (Manuscript **Received** February 2,
 2005; **Revised** June 13, 2005)

- $\Delta \xi$: Incremental martensite volume fraction of the fibers
- A_f : Austenite finish temperature
- A_s : Austenite start temperature
- C_A : Slope of stress and temperature curve for martensite to austenite transformation
- C_f : Stiffness matrix of the fiber
- C_M : Slope of stress and temperature curve for austenite to martensite transformation
- \mathbf{e}^{TR} : Transformation strain in vector notation
- f : Volume fraction of fibers
- M_f : Martensite finish temperature
- M_s : Martensite start temperature

Matrix

- ε^P : Plastic strain along fiber direction
- $\Delta \varepsilon^P$: Small increment of the plastic strain
- σ_{my} : Yield stress of the matrix
- $\sigma_{m,0}, K, n$: Constants of Ludwick equation for work-hardening matrix
- $\Delta \sigma_{my}$: Increase in the yield stress of the matrix due to the small increment of the plastic strain
- C_m : Stiffness matrix of the matrix material
- \mathbf{e}^P : Plastic strain in vector notation

1. Introduction

Shape memory alloys (SMAs) have been well known to have three dominant properties such as shape memory effect (SME), pseudoelasticity, and high damping capacity (Liu et al., 1999; Furuya et al., 1993; Taya et al., 1995). SMA fiber reinforced composites (SMA composites) have been processed to use the SME of SMA, resulting in better mechanical properties than unreinforced matrix materials such as yield stress and fracture toughness at high in-use temperatures (Liu et al., 1999; Furuya et al., 1993; Taya et al., 1995; Hamada et al., 1998; Park et al., 2002; Park and Lee, 2004). It is well known that the compressive residual stress in the matrix due to the reverse transformation of SMA fibers from martensite to austenite state enhances the tensile properties of

SMA composites.

To shape-memorize the SMA in the composite, the composite has been loaded and unloaded at certain temperatures (Furuya et al., 1993; Taya et al., 1995; Hamada et al., 1998; Park et al., 2002; Park and Lee, 2004), which is called a prestraining process. The permanent strain is then induced in the composite during shape memory process, which is called a prestrain. Prestrain is known to define the shape memory amount given to the composite, and it has been used as a key design parameter for the SMA composite.

Two shape memory processes have been proposed and utilized throughout the literatures (Furuya et al., 1993; Taya et al., 1995; Hamada et al., 1998; Park et al., 2002; Park and Lee, 2004). The one is a stress-induced transformation of SMA from twinned martensite to detwinned martensite at temperatures lower than martensite start temperature (Furuya et al., 1993; Taya et al., 1995; Park et al., 2002; Park and Lee, 2004), while the other is a stress-induced transformation of SMA from austenite to detwinned martensite at temperatures between martensite start temperature and austenite start temperature (Hamada et al., 1998). The increases in yield stress of the composite have been experimentally (Furuya et al., 1993; Taya et al., 1995; Hamada et al., 1998; Park et al., 2002; Park and Lee, 2004) and theoretically (Taya et al., 1995; Hamada et al., 1998; Yamada et al., 1993; Cherkaoui et al., 2000; Lee et al., 2001; Auricchio et al., 2003) observed by using the two mechanisms. Since the prestrain in the composite is the sum of the strain due to phase transformation of the SMA and plastic strain in the matrix, the amount of phase transformation of SMA and plastic strain need to be distinguished for the prediction of tensile properties of the composite. In addition, residual stress in the matrix generated during shape memory process plays a role in strengthening of the composite. However, a detailed research on a comparison between the two shape memory processes has not been performed in terms of the prestrain, shape memory amount, plastic strain, and residual stress, respectively.

Since a mass production of the composite can

be accomplished by using discontinuous SMA fibers, discontinuous SMA fiber reinforced aluminum matrix composite has been chosen as a model composite for the analysis. The shape memory process based on austenite state of SMA has been published elsewhere (Lee et al., 2004). In this study, this model has been extended to be applicable to the composite with initially martensitic state of the SMA fibers. Eshelby's equivalent inclusion method (Eshelby, 1957) with Mori-Tanaka's mean field theory (Mori and Tanaka, 1973) is used to compute the plastic deformation of the matrix and the residual stresses and strains in both the matrix and fiber generated by the shape memory processes. The detailed states of the SMA fibers and the matrix by the two shape memory processes are presented and compared.

2. Analytical Model

In the present model, a phenomenological model is used to describe the constitutive equations of the SMA fibers, where a cosine-type equation is employed for the transformation of the SMA (Liang and Rogers, 1990). It is noted that both stress and strain components are expressed by 1×6 column vectors, and all vectors are designated in bold-face.

2.1 Shape memory processes

As schematically shown in Fig. 1, the path of the phase transformation of SMA depends on the temperature and stress. The temperature determines the initial state of SMA before applying load. The SMA is transformed from twinned martensite to detwinned martensite below martensite start temperature (M_s), while the SMA is transformed from austenite to detwinned martensite above M_s . Although experimental results (Dye, 1990) have shown that stresses for the initiation and termination of phase transformation of SMA slightly increase as temperature decreases below M_s , it is assumed for simplicity that the critical stress values below M_s is constant and denoted by σ_{ams} and σ_{amf} , which means the critical stresses at the start and the finish of the

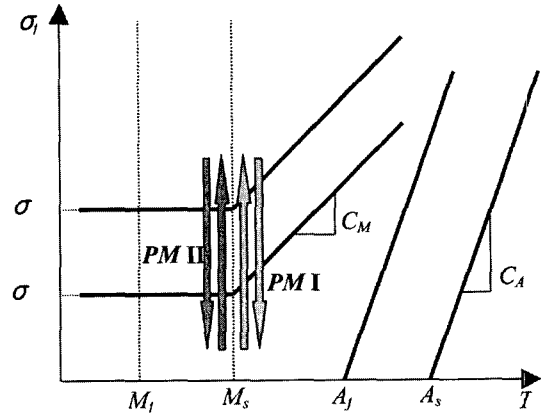


Fig. 1 Critical stresses for transformation or martensite twin conversion as functions of temperature and stress (Brinson, 1993)

conversion of the martensitic variants, respectively (Brinson, 1993). The two shape memory processes are divided into the prestraining mechanisms I and II, which are explained below.

2.1.1 Prestraining mechanism I (PM I)

Consider the SMA in full austenite at temperatures between M_s and A_s (austenite start temperature). Loading the composite under this temperature range, the SMA is transformed from austenite to detwinned martensite by stress-induced transformation. After unloading the composite, the transformed state is still maintained. For simplifying comparison between the shape memory processes by neglecting temperature effect, the temperature of the composite is assumed to be just higher than M_s . Since the SMA is assumed to be initially 100% austenite, the detwinned martensite volume fraction of the SMA, ξ_{A-DTM} , during the transformation is simply expressed as (Brinson, 1993)

$$\xi(T, \sigma_f)_{A-DTM} = \frac{1}{2} \cos \left\{ \frac{\pi [\sigma_f - \sigma_{dmf} - C_M (T - M_s)]}{\sigma_{dms} - \sigma_{dmf}} \right\} + \frac{1}{2} \quad (1)$$

where T , σ_f , and C_M denote the temperature, effective stress, and the slope of stress and temperature curve for austenite to martensite transformation of the SMA fibers, respectively.

2.1.2 Prestraining mechanism II (PM II)

Consider the SMA in fully twinned martensite at lower temperatures than M_s . Increasing the applied load to the composite, the SMA is transformed from twinned martensite to detwinned martensite. For neglecting temperature effect, the temperature of the composite is assumed to be just lower than M_s . Assuming there is no single variant martensite at initial state of SMA, the detwinned martensite volume fraction, ξ_{TM-DTM} , is a simple function of stress only and is given as follows (Brinson, 1993).

$$\xi(\sigma_f)_{TM-DTM} = \frac{1}{2} \cos \left[\frac{\pi(\sigma_f - \sigma_{dmf})}{\sigma_{dms} - \sigma_{dmf}} \right] + \frac{1}{2} \quad (2)$$

The phase transformation strain of the fibers, \mathbf{e}^{TR} , due to the SME for both mechanisms can be expressed as

$$\begin{aligned} \mathbf{e}^{TR} &= \varepsilon^{TR} \Delta \xi [-\nu_f \quad -\nu_f \quad 1 \quad 0 \quad 0 \quad 0] \\ &= \varepsilon^{TR} \Delta \xi \mathbf{V}^{TR} \end{aligned} \quad (3)$$

where ε^{TR} and ν_f denote the phase transformation strain from austenite to detwinned martensite or from twinned martensite to detwinned martensite and the Poisson's ratio of the fiber, respectively. $\Delta \xi$ is the incremental martensite volume fraction of the fibers, which is a function of temperature and stress.

2.2 Constitutive equations

Three-dimensional constitutive equations are derived for computing the stress and strain in the SMA metal matrix composite by using Eshelby's equivalent inclusion method (Eshelby, 1957) with the Mori-Tanaka mean field theory (Mori and Tanaka, 1973). The model composite is assumed to be reinforced by short fibers aligned in the direction of x_3 for simplicity of analysis. The shaded areas in Fig. 2 represent the SMA fibers, and unshaded area does matrix material.

The matrix and fibers are initially in elastic state. By increasing an applied load, the plastic strain, \mathbf{e}^P , is generated in the matrix and is expressed as

$$\mathbf{e}^P = \varepsilon^P [-0.5 \quad -0.5 \quad 1 \quad 0 \quad 0 \quad 0] = \varepsilon^P \mathbf{V}^P \quad (4)$$

where ε^P denote the plastic strain along x_3 . The

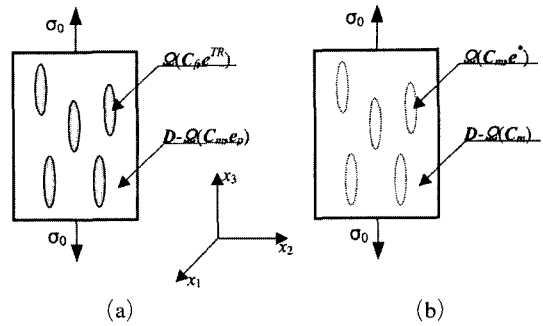


Fig. 2 Analytical model for calculating residual stresses and strains in both SMA fiber and metal matrix, (a) original problem, which is converted to (b) Eshelby's equivalent inclusion problem

yield stress of the matrix, σ_{my} , and the increase in the yield stress of the matrix, $\Delta \sigma_{my}$, due to the small increment of the plastic strain, $\Delta \varepsilon^P$, are expressed as follows.

$$\sigma_{my} = \sigma_{my,0} + K(\varepsilon^P)^n \quad (5)$$

$$\Delta \sigma_{my} = nK(\varepsilon^P)^{n-1} \Delta \varepsilon^P \quad (6)$$

The original problem is shown in Fig. 2(a), where the phase transformation strain is given to SMA fibers and the plastic strain is given to the matrix. Superimposing $-\mathbf{e}^P$ into the whole composite domain and converting to the Eshelby's equivalent inclusion problem, the phase transformation and plastic strains are given to the SMA fibers shown in Fig. 2(b). A stress σ_o with components $\sigma_o[0 \ 0 \ 1 \ 0 \ 0 \ 0]$ is applied in the direction of x_3 (along the fiber direction) for generating the prestrain.

By using Eshelby's inclusion method with the Mori-Tanaka mean field theory, the average stress inside the fibers can be expressed as

$$\begin{aligned} \sigma_o + \sigma &= C_f \cdot (\mathbf{e}_o + \bar{\mathbf{e}} + \mathbf{e} - \mathbf{e}^{TR} + \mathbf{e}^P) \\ &= C_m \cdot (\mathbf{e}_o + \bar{\mathbf{e}} + \mathbf{e} - \mathbf{e}^*) \end{aligned} \quad (7)$$

where C , \mathbf{e}_o , $\bar{\mathbf{e}}$, \mathbf{e} , \mathbf{e}^* represent the stiffness matrix, the strain generated in the matrix without the inhomogeneity by applied stress, the average elastic strain in the matrix domain, strain disturbed by the existence of the inhomogeneity, and the equivalent eigenstrain of the equivalent in-

clusion, respectively. Subscripts m and f represent the matrix and fiber, respectively. Young's modulus of the fibers, E_f , depends on the martensite volume fraction, ξ , and is also assumed to be linear function of ξ .

From the requirement that the integration of disturbed stress over the entire composite domain must vanish, $\bar{\mathbf{e}}$ is given as

$$\bar{\mathbf{e}} + f(\mathbf{e} - \mathbf{e}^*) = \mathbf{0} \quad (8)$$

where f is the volume fraction of the fibers. The total strain \mathbf{e} in the fiber is related through Eshelby's tensor \mathbf{S} as follows.

$$\mathbf{e} = \mathbf{S} \cdot \mathbf{e}^* \quad (9)$$

From Eqs. (7) ~ (9), the average stresses in the fiber and matrix, $\langle \boldsymbol{\sigma} \rangle_f$ and $\langle \boldsymbol{\sigma} \rangle_m$, can be computed as

$$\langle \boldsymbol{\sigma} \rangle_f = [\mathbf{I} + \mathbf{RF}] \cdot \boldsymbol{\sigma}_o + \mathbf{RE} \cdot (\mathbf{e}^{TR} - \mathbf{e}^P) \quad (10)$$

$$\langle \boldsymbol{\sigma} \rangle_m = \left[\mathbf{I} - \frac{f}{1-f} \mathbf{RF} \right] \cdot \boldsymbol{\sigma}_o - \frac{f}{1-f} \mathbf{RE} \cdot (\mathbf{e}^{TR} - \mathbf{e}^P) \quad (11)$$

where

$$\begin{aligned} \mathbf{RF} &= (1-f) \mathbf{C}_m \cdot (\mathbf{S} - \mathbf{I}) \\ &\cdot \{ (\mathbf{C}_f - \mathbf{C}_m) \cdot [(1-f) \mathbf{S} + f \mathbf{I}] + \mathbf{C}_m \}^{-1} \quad (12) \\ &\cdot (\mathbf{C}_m - \mathbf{C}_f) \cdot \mathbf{C}_m^{-1} \end{aligned}$$

$$\begin{aligned} \mathbf{RE} &= (1-f) \mathbf{C}_m \cdot (\mathbf{S} - \mathbf{I}) \\ &\cdot \{ (\mathbf{C}_f - \mathbf{C}_m) \cdot [(1-f) \mathbf{S} + f \mathbf{I}] + \mathbf{C}_m \}^{-1} \cdot \mathbf{C}_f \quad (13) \end{aligned}$$

It is noted that bold face \mathbf{RF} , \mathbf{RE} , \mathbf{I} , and \mathbf{C}_i are 6×6 matrices and \mathbf{I} is identity matrix.

By superimposing \mathbf{e}^P into the whole domain of the composite, the total strains in the fiber and matrix, \mathbf{e}_f and \mathbf{e}_m , are given by

$$\mathbf{e}_m = \mathbf{e}_o + \bar{\mathbf{e}} + \mathbf{e}^P \quad (14)$$

$$\mathbf{e}_f = \mathbf{e}_o + \bar{\mathbf{e}} + \mathbf{e} + \mathbf{e}^P \quad (15)$$

The volume average of the strain induced in the entire composite is computed by using Eqs. (14) and (15), and is expressed as

$$\mathbf{e}_c = \mathbf{C}_m^{-1} \cdot \boldsymbol{\sigma}_o + f \mathbf{e}^* + \mathbf{e}^P \quad (16)$$

where

$$\begin{aligned} \mathbf{e}^* &= \{ (\mathbf{C}_f - \mathbf{C}_m) \cdot [(1-f) \mathbf{S} + f \mathbf{I}] + \mathbf{C}_m \}^{-1} \\ &\cdot \{ (\mathbf{C}_m - \mathbf{C}_f) \cdot \mathbf{C}_m^{-1} \cdot \boldsymbol{\sigma}_o + \mathbf{C}_f \cdot (\mathbf{e}^{TR} - \mathbf{e}^P) \} \quad (17) \end{aligned}$$

The strain along x_3 direction induced in the composite after unloading is the third component of Eq. (16), which is the prestrain.

2.2 Computation procedures

Based on the derived equations in section 2.1 and 2.2, the numerical analysis has been conducted by changing applied load incrementally. The entire processes for computation are explained below in detail for the *PM I* and those for the *PM II* are omitted because it is the same process.

The load to the composite is increased until the matrix starts to yield. Without the plastic strain, \mathbf{e}^P , the amount of phase transformation of SMA, \mathbf{e}^{TR} , is computed by using Eqs. (1), (3), (10) and (11). Further increasing the applied load, \mathbf{e}^{TR} and \mathbf{e}^P are computed with Eqs. (1), (3), (5), (6), (10), and (11). The fiber stress and matrix stress are converted into the effective stresses for determining the transformation of the fiber and the plastic strain in the matrix. After reaching a target applied stress, the composite is fully unloaded, during which further stress-induced martensitic transformation does not occur. The total strain in the composite remained after loading and unloading processes is computed by using Eq. (16), which is defined as the prestrain given to the composite.

3. Results and Discussions

The material properties of the model composite are tabulated in Table 1, which are used for the present computation. The matrix material behaves as strain-hardening of the power-law type, and the fibers deform super-elastically.

The shape memory amount is defined as the twinned martensite volume fraction, transformed from detwinned martensite or austenite during a prestraining process. Predicted results are plotted as a function of the prestrain and are shown in Fig. 3. Increasing the applied load, the phase transformation of SMA takes place with the elastic deformation of the matrix. During this period, the prestrain mostly comes from the phase transformation of SMA. As shown in Fig. 3(a),

the shape memory amounts induced by *PM I* and *PM II* increase rapidly as the prestrain goes up to the points of 2.3×10^{-4} and 10^{-6} , respectively. These prestrains represent the onset point of the matrix yielding. Since the fibers under *PM II* are softer than those under *PM I* as shown in Table 1, the matrix material by *PM II* reaches yield stress at lower prestrain compared with *PM I*.

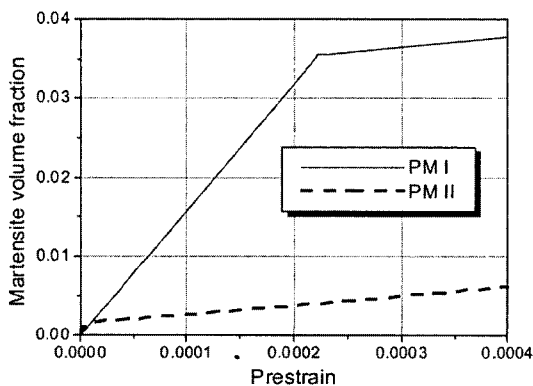
After reaching the matrix yield point, the phase transformation of SMA and the plastic deformation of the matrix occur simultaneously. Since the prestrain is the sum of the transformation strain of the fibers and the plastic strain in the matrix, the amount of shape memory gradually increases as the prestrain increases. At the prestrain of 0.073, the SMA is transformed from twinned martensite

or austenite to 100% detwinned martensite. In a small prestrain region, the shape memory amount induced by *PM I* is slightly higher than that by *PM II*. However, in a few percent prestrain region, which has been used for examining the effect of the prestrain on the strengthening mechanism of the composite in the literatures (Furuya et al., 1993; Taya et al., 1995; Hamada et al., 1998; Park et al., 2002; Park and Lee, 2004), the shape memory amounts induced by both *PM I* and *PM II* show almost the same level. That is, the shape memory amount in this range is not greatly influenced by the prestraining mechanisms.

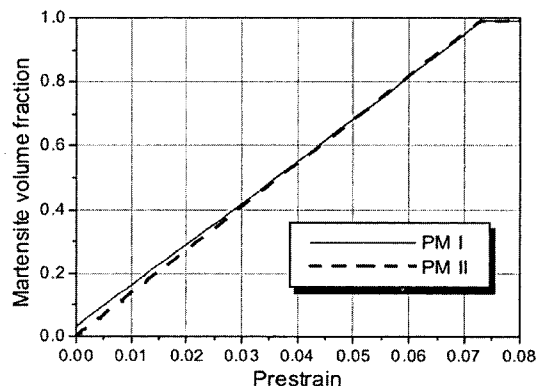
The plastic strains built in the matrix after the prestraining processes are predicted and are shown in Fig. 4 as a function of the prestrain. As

Table 1 Material Properties (Hamada et al., 1998; Brinson et al., 1993)

		6061 Aluminum	TiNi fiber	
			Austenite	Martensite
Young's modulus [GPa]		70	67	26.3
Poisson ratio		0.33	0.43	
Yield stress	$\sigma_{my,0}$ [MPa]	245		
	K [MPa]	85		
	n	0.2		
Fiber volume fraction, <i>f</i>			10%	
Aspect ratio			5	
Transformation strain			0.067	
Transformation temperatures [°C]			$M_f=9, M_s=18.4, A_s=34.5, A_f=49$	
Critical stress [MPa]			$\sigma_{dms}=100, \sigma_{dmf}=170$	
Slope [MPa/°C]			$C_M=8, C_A=13.8$	



(a) Small prestrain region



(b) Whole prestrain region

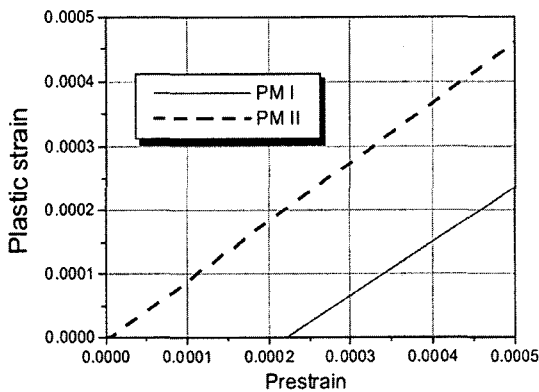
Fig. 3 Martensite volume fraction of shape memory alloy fiber as a function of prestrain

shown in Fig. 4(a), the plastic strain by *PM II* is first generated and its magnitude is higher than that by *PM I*. The fibers by *PM I* are stiffer than those by *PM II*, so the fibers by *PM I* carry more load than those by *PM II*. The fibers by *PM I* reach the onset point of phase transformation with relatively low applied stress. The fibers by *PM I* are first phase-transformed to generate the prestrain without the plastic deformation of the matrix. The fibers by *PM II*, however, are much softer than the matrix material, so the matrix carries more load than the fibers do. Thus, when load is applied, the matrix of *PM II* deforms plastically earlier compared with *PM I*, as shown in Fig. 4(a).

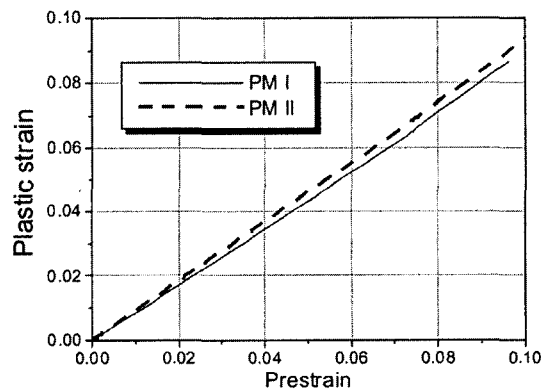
The plastic strains by *PM II* are higher over the whole prestrain range than those by *PM I*. Con-

sider the composite with the prestrain of 5%. As shown in Fig. 3(b), the strains due to the phase transformation by both *PM I* and *PM II* are almost the same (≈ 0.68), at this prestrain. In addition to the phase transformation strain and the plastic strain, the prestrain is known to be a function of the material constants from Eqs. (16) and (17). The softer fibers by *PM II* have smaller e^* , resulting in smaller e^* of the composite. The plastic strain in the matrix by *PM II* has larger magnitude, comparing with *PM I*. At the same prestrain value, therefore, the prestraining process with the softer fibers, *PM II*, is more favorable to strengthen the composite due to higher plastic strain than *PM I*.

The relationship between the prestrain and applied stress is shown in Fig. 5. The prestrain by

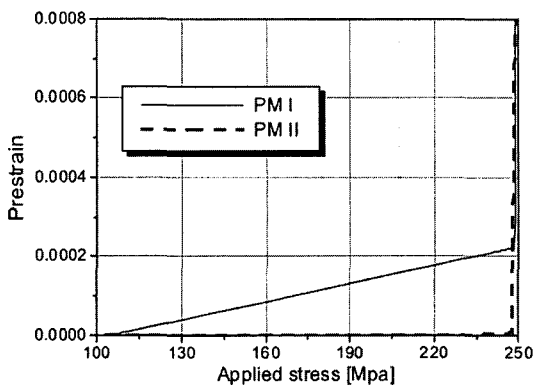


(a) Small prestrain region

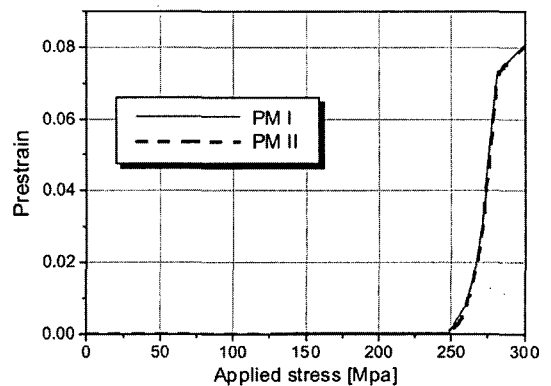


(b) Whole prestrain region

Fig. 4 Plastic strain in the matrix as a function of prestrain



(a) Small prestrain region



(b) Whole prestrain region

Fig. 5 Prestrain in the composite as a function of an applied stress

PM I starts to be built up when the applied stress is around 105 MPa, while the prestrain by *PM II* starts to build up around the applied stress of 238 MPa. The fibers by *PM I* are stiffer than those by *PM II*, so the fibers by *PM I* carry more load to be transformed at smaller applied load. The magnitude of the applied stress to generate the same prestrain of a few percentage is almost the same for both *PM I* and *II*.

The residual stresses in the matrix are computed in terms of effective stress, $\langle \sigma \rangle_{m,3} - \langle \sigma \rangle_{m,1}$, and plotted as a function of the prestrain. As shown in Fig. 6, the residual stress in the matrix by *PM II* is compressive over all the prestrain region and becomes more compressive as the prestrain increases. However, the residual stress in the matrix by *PM I* is tensile up to the prestrain of 0.06, beyond which it becomes compressive. Whenever the same prestrain is given to the composite by both *PM I* and *II*, the residual stress in the matrix by *PM II* is more compressive. Thus, the yield stress of the composite by *PM II* would be higher than that by *PM I*.

The residual stress in the matrix by *PM I* is tensile in a small prestrain region after the prestraining process, while those by *PM II* are nearly zero. As shown in Fig. 3, martensite volume fraction by *PM I* increases faster at the same prestrain than that by *PM II*. Since fiber stress is relaxed due to the stress-induced transformation of the fibers, the matrix stress becomes more tensile after loading. The matrix stress by *PM I*

becomes more tensile than *PM II* after fully unloading.

As the prestrain increases further, the residual stresses in the matrix by *PM I* and *II* become smaller. During this period, both the phase transformation of the fiber and plastic deformation of the matrix take place simultaneously. The relaxation of the matrix stress by the plastic deformation is larger than that by the phase transformation, so the matrix stress becomes more compressive with the increase of the prestrain. When the prestrain reaches 0.073, the transformation of the fiber is completed, as shown in Fig. 3. Beyond this point, the fibers are in fully detwinned martensite state, and the matrix deforms plastically. As further prestraining the composite beyond this point, the residual stress in the matrix becomes more compressive.

The strengthening of the SMA composite is known to be mainly dependent on the residual stress generated in the matrix during prestraining process as well as the stress in the matrix due to the shape recovery of SMA. For the composites with the same prestrain of a few percentage by *PM I* and *II*, the yield stress of the composite by *PM II* would be higher than that by *PM I* owing to the compressive residual stress in the matrix.

4. Conclusions

The two shape memory processes, austenite to detwinned martensite transformation (Prestrain Mechanism I) and twinned martensite to detwinned martensite transformation (*PM II*) of the shape memory alloy, for discontinuous TiNi shape memory alloy reinforced aluminum matrix composite have been modeled and theoretically investigated. It is shown that the two shape memory processes do not crucially affect the shape memory amount in the composite with the same prestrain except for very small prestrain region. In this region, the fibers by *PM I* are more phase-transformed. The magnitude of the applied stress to generate the same prestrain is almost the same for the two shape memory processes, while phase transformation of fibers initiates at smaller applied load by *PM I* than by *PM II*. Larger

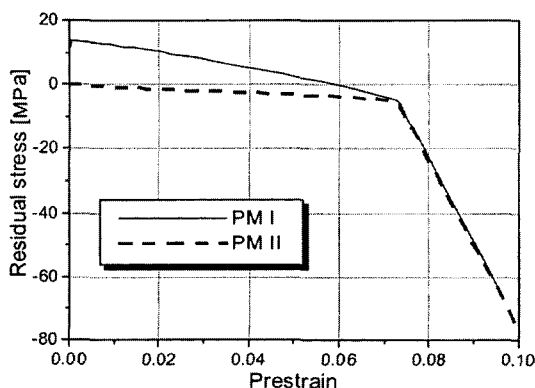


Fig. 6 Residual stress in the matrix as a function of prestrain

plastic strain and higher compressive stress in the matrix have been predicted by the *PM II*. Based on the results through this study, it can be concluded that the *PM II* would be helpful to increase further the yield stress of the composite owing to the compressive residual stress and large plastic strain in the matrix as well as the intrinsic shape memory effect of the shape memory alloy.

References

- Auricchio, A., Marfia, S. and Sacco, E., 2003, "Modeling of SMA Materials : Training and Two way Memory Effects," *Computers and Structures*, Vol. 81, pp. 2301~2317.
- Brinson, L. C., 1993, "One-Dimensional Constitutive Behavior of Shape Memory Alloys: Thermomechanical Derivation with Non-Constant Material Functions and Redefined Martensite Internal Variable," *J. Intell. Material Syst. and Struct.*, Vol. 4, pp. 229~242.
- Cherkaoui, M., Sun, Q. P. and Song, G. Q., 2000, "Micromechanics Modeling of Composite with Ductile Matrix and Shape Memory Alloy Reinforcement," *Int. J. of Solids and Structures*, Vol. 37, pp. 1577~1594.
- Dye, T. E., 1990, "An Experimental Investigation of the Behavior of Nitinol," MS thesis, Virginia Tech.
- Eshelby, J. D., 1957, "The determination of the Elastic Field of an Ellipsoidal Inclusion, and Related Problems," *Proc. of the Royal Society of London*, Vol. A241, pp. 376~396.
- Furuya, Y., Sasaki, A. and Taya, M., 1993, "On Enhanced Mechanical Properties of TiNi Shape Memory Fiber/Al Matrix Composite," *Mater. Trans. JIM*, Vol. 34, pp. 224~227.
- Hamada, K., Lee, J. H., Mizuuchi, K., Taya, M. and Inoue, K., 1998, "Thermomechanical Behavior of TiNi Shape Memory Alloy Fiber Reinforced 6061 Aluminum Matrix Composite," *Metallurgical and Materials Trans.*, Vol. 29A, pp. 1127~1135.
- Lee, W. B., Jie, M. and Tang, C. Y., 2001, "Constitutive Modeling of Aluminum Matrix NiTi Fiber-Reinforced Smart Composite," *J. of Materials and Processing Technology*, Vol. 116, pp. 219~223.
- Lee, J. K., Kim, J. G. and Kim, G. D., 2004, "An Analytical Study on Prestrain and Shape Memory Effect of Composite Reinforced with Shape Memory Alloy," *The Korean Society for Composite Materials*, Vol. 17, No. 5, pp. 54~60.
- Liang, C. and Rogers, C. A., 1990, "One-Dimensional Thermomechanical Constitutive Relations for Shape Memory Materials," *J. of Intell. Mater. Syst. and Struct.*, Vol. 1, No. 2, pp. 207~234.
- Liu, Y., Li, Y., Ramesh, K. T. and Humbeek, J. V., 1999, "High Strain Rate Deformation of Martensitic NiTi Shape Memory Alloy," *Scripta Materialia*, Vol. 41, No. 1, pp. 89~95.
- Mori, T. and Tanaka, K., 1973, "Average Stress in the Matrix and Average Elastic Energy of Materials with Misfitting Inclusions," *Acta Metallurgica*, Vol. 21, pp. 571~574.
- Park, Y. C., Park, D. S., Lee, J. H. and Lee, G. C., 2002, "Fabrication and Characterization of TiNi Shape Memory Alloy Fiber Reinforced 6061 Aluminum Matrix Composite by Using Hot Press," *Trans. KSME A*, Vol. 26, No. 7, pp. 1223~1231.
- Park, Y. C. and Lee, J. K., 2004, "Fabrication and AE Characteristics of TiNi/Al6061 Shape Memory Alloy Composite," *KSME Int. J.*, Vol. 18, No. 3, pp. 453~459.
- Taya, M., Shimamoto, A. and Furuya, Y., 1995, "Design of Smart Composites Based on Shape Memory Effect," *Proc. of ICCM-10*, Vol. 5, pp. 275~282.
- Yamada, Y., Taya, M. and Watanabe, R., 1993, "Strengthening of Metal Matrix Composite by Shape Memory Effect," *Mater. Trans. JIM*, Vol. 34, No. 3, pp. 254~260.